Available online at www.sciencedirect.com

ScienceDirect

Procedia Structural Integrity 2 (2016) 3539–3545

Structural Integrity Procedia

www.elsevier.com/locate/procedia

21st European Conference on Fracture, ECF21, 20-24 June 2016, Catania, Italy

Tensile mechanical performance of electron-beam welded joints from aluminum alloy (Al-Mg-Si) 6156

Nikolaos D. Alexopoulos[a,*], Theano N. Examilioti[a], Vasilis Stergiou[b], Stavros K. Kourkoulis[c]

[a]*Department of Financial Engineering, University of the Aegean, 82 132 Chios, Greece*
[b]*Special Processes & Laboratories Depaartment, Hellenic Aerospace Industry, 320 09 Schimatari, Greece*
[c]*Laboratory of Testing and Materials, Section of Mechanics, National Technical University of Athens, 9 Heroes Polytechniou Str., 15780 Athens, Greece*

Abstract

The mechanical behavior of both, reference and electron beam welded aluminum alloy 6156 specimens was experimentally investigated. Sheets of AA6156 were artificially aged before and after the welding process and tensile specimens were machined from the welded sheets according to the ASTM E8 standard. The specimens were artificially aged at 170ºC for different times that corresponded to all precipitation-hardening conditions, namely under-ageing (UA), peak-ageing (PA) and over-ageing (OA). The results showed that the effect of welding without any heat treatment (condition T4) decreases by, about 100 MPa, the yield stress and the yield strength, while the remaining elongation at fracture hardly exceeds 4 %. It was also shown that artificial ageing before welding increases the tensile ductility (almost 50 % joint efficiency in deformation) while the artificial ageing post to welding significantly increases the strength properties (more than 75 % joint efficiency in strength).

Peer-review under responsibility of the Scientific Committee of ECF21.

Keywords: tension; aluminum alloy; heat treatment; welding; precipitation-hardening;

* Corresponding author. Tel.: +0030-22710-35464; fax: +0030-22710-35429.
E-mail address: nalexop@aegean.gr

Peer review under responsibility of the Scientific Committee of ECF21.
10.1016/j.prostr.2016.06.441

1. Introduction

Aluminum alloys from the 6xxx series, e.g. 6056, were already selected in fuselage sections where improved strength properties and damage-tolerance capabilities are required. Nevertheless, future metallic airframes may contain welded structures to achieve lightweight integral airframes, e.g. Airbus A380, in order to remove the classical riveted joints. Innovative 6156 fuselage sheets are particularly recommended for such applications as an impression of having higher damage tolerance capabilities than its predecessors, e.g. Lequeu et al. (2007). In addition, the good weldability, low density and corrosion resistance made this alloy more attractive for widespread usage in aircraft applications. AA6156 has already been used to the lower shell and the hollow sections of the lower fuselage of aircrafts, mainly due to its high weldability potential, e.g. Dif et al. (2000). Laser and electron beam welding have been widely applied in the industry due to their great advantages that ensure narrow heat affected zone, small distortion and relatively high welding speed than traditional welding processes.

So far the literature review on the aluminum alloy 6156 remains rather limited; the effect of ageing treatments on microstructure and hardness are reported by Lin et al. (2012) and Jin et al. (2011), while the effects of Ag addition on the long thermal stability of this alloy were reported by Zhang et al. (2012). She at al. (2012) reported the high cycle fatigue performance of the alloy while Morgeneyer et al. (2006) and (2008) investigated the quench sensitivity of toughness of this alloy. In the present work, tensile tests on electron beam welded specimens from AA6156 having different artificial ageing heat treatment before and after the welding process will be carried out. The goal of this article is to provide useful information regarding precipitation sequence and their effect on the tensile mechanical behavior of the welded joints.

2. Material and experiments

AA6156 sheets of 3.6 mm nominal thickness were joined by electron beam welding (EBW) in various heat treatment artificial ageing conditions. The workflow of the present work is summarized in three different batches that can be seen in Fig. 1.

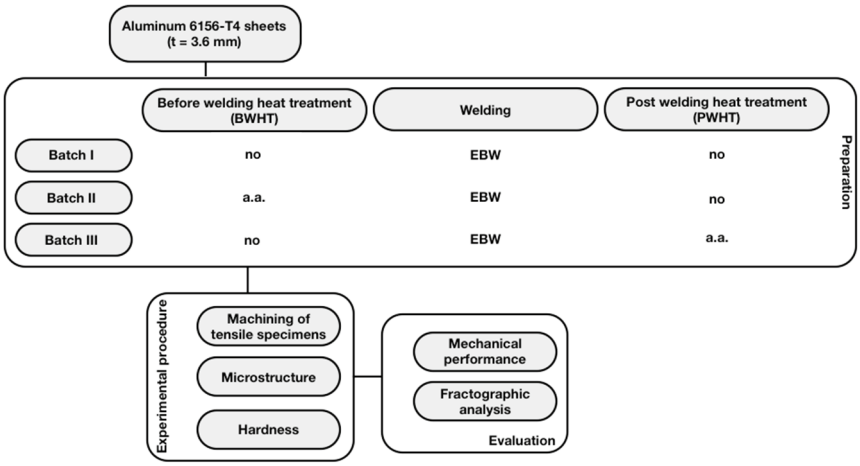

Fig. 1. Process flow diagram of the performed work in this article.

2.1. Material

The material used for the present investigation was 6156 wrought aluminum alloy in T4 condition that was received in sheet form with nominal thickness of 3.6 mm and without any surface corrosion protection (Alclad). The sheets had geometrical dimensions of 35 x 50 cm, while their thickness is typical for aircraft structures. The weight percentage chemical composition of the alloy is: Si 0.7-1.3%-Mg 0.6-1.2% - Cu 0.7-1.1% - Mn 0.4-0.7% - Fe <0.2% - Cr <0.25% - Zn 0.1-0.7% - Al remainder.

2.2. Welding of the sheets

Several full penetration welds were performed without using filler wire. Before the butt-welding procedure, five equally positioned tack welds were made to first assemble the sheets in order to be welded. Electron beam welding parameters used were: current was selected to be equal to 95 mA, the beam focus was 6.90 A, while the speed was about 1650 mm/min. After the welding process, the sheets were released from the fixture and were cooled down to room temperature. Visual inspection was used to determine the outer appearance of the weld seam, especially for weld imperfections such as incomplete filled grooves and undercutting of the weld seam. In addition, X-ray inspection was used to determine the existence of several inner imperfections such as porosity and cracks. No structural defects were detected, while the microstructural properties of the joints were investigated by hardness measurements as well as optical microscopy.

2.3. Artificial ageing and manufacturing of tensile specimens

The sheets were surface cleaned with alcohol and then were artificially aged (heat treated) in an electric oven with air circulation Elvem (2600 W) with ± 0.1ºC temperature control. Artificial ageing conditions were performed at 170ºC and for different ageing times. Tensile specimens were machined from the longitudinal (L) direction of the sheets, according to the ASTM E8 specification with 12.5 mm x 3.6 mm being the reduced cross-section and 50 mm being the gauge length of the specimens. For the welded specimens, twenty-six tensile specimens were machined from the sheets, 8 without any heat treatment and 18 with different artificial ageing heat treatment, Table 1. Some specimens were artificially aged before the welding process (hereafter will be called as Before Welding Heat Treatment - BWHT) and some specimens were artificially aged post to the welding process (hereafter will be called as Post to Welding Heat Treatment - PWHT). Three artificial ageing times were selected from Stefanou et al. (2014) to artificially age the material at all available ageing conditions, including Under-Ageing (UA), Peak-Ageing (PA) and Over-Ageing (OA). Machining of the specimens and their surface preparation was implemented according to the same ASTM standard; attention was paid to manufacture the welded specimens with the fusion zone area being in the middle of the reduced cross-section area of the specimens. This was essential in order to compare the mechanical behavior of the welded joints against the respective unwelded specimens.

Table 1. Experimental test matrix and respective number of tensile test specimens.

Temperature		Artificial ageing **before** electron beam welding (BWHT)			# of specimens
		4 h	**28 h**	**96 h**	
		3 sp.	3 sp.	3 sp.	
170 ºC	**0 h** 8 sp.	Artificial ageing **post** to electron beam welding (PWHT)			
		4 h	**28 h**	**96 h**	
		3 sp.	3 sp.	3 sp.	
Total	8 sp.	6 sp.	6 sp.	6 sp.	26 sp.

2.4. Microstructure of the welded joints

For the metallographic examination, specimens were sectioned transversely to the welding direction. The specimens for hardness measurements were ground flat and the testing surfaces were finished with 1000 grit SiC paper. Microhardness was measured using a 200 gf load, dwell time for 5 sec and typical pyramid indenter for Vickers hardness measurements ($HV_{0.2}$). The measurements points were selected to be at the middle thickness of the specimens (1.8 mm in depth) and came across the areas of base metal (BM), heat affected zone (HAZ) and fusion zone (FZ) that were well marked on the respective results diagrams.

2.5. Mechanical testing

Tensile tests were carried out in a servo-hydraulic Instron 8801 100 kN loading frame. The mechanical tests were conducted according to ASTM E8 specification and the strain rate was kept constant and equal to 0.833 sec^{-1}. At

least three specimens were tested per different case in order to get reliable average data (Table 1). In order to enable recording of the deformation of the welded joints, an extensometer with gauge length 12.5 mm was attached at the reduced cross-section of the tensile specimen to record solely the deformation of the welded joint. A data logger was used during the experimental testing time and the recorded values of axial load, displacement and nominal strain were stored in a computer.

3. Results and discussion

The test results are reported in this section. The microstructure of the reference alloy 6156 at the T4 condition corresponds to aluminum grains, eutectical silicon particles and some formed second phase particles (β'' phase with stoichiometric analogy Mg: 2 Si: 1). These particles are being precipitated by the artificial ageing heat treatment as a strengthening phase to increase the strength capabilities of AA6156 on the expense of tensile ductility. During the welding process, these precipitates were dissoluted (solid solution) in the aluminum matrix of the melt zone area (Fusion Zone - FZ) and therefore the respective volume area has no formed precipitates. The solutionized material in FZ exhibits low strength and essential ductility properties due to the absence of these precipitates. Preliminary results showed that due to the high-speed thawing (characteristic of electron beam welding method) it is possible that some precipitates remain in the microstructure of the material in the form of acicular crystals. There is also, a slight growth of precipitates in the heat-affected zone of the weld due to the heat transfer from the weld fusion zone.

3.1. Hardness measurements

Fig. 2 shows the Vickers microhardness measurements across the weld and reveals the essential hardness decrease in the fusion zone of the welded joints. This was noticed for both cases, when artificial ageing was applied, before (Fig. 2a) or post to the welding process (Fig. 2b). For the latter case, hardness was slightly increased in the fusion zone as well as in the fine-grained heat affected zone as a sequence of the precipitation of the second-phase particles due to artificial ageing. It is also worth noticing the hardness fluctuations within the HAZ, perhaps due to the different precipitation microstructure (fine dispersion near FZ against coarsening near BM). Microstructure and hardness measurements will be linked and further analyzed in a follow-up article.

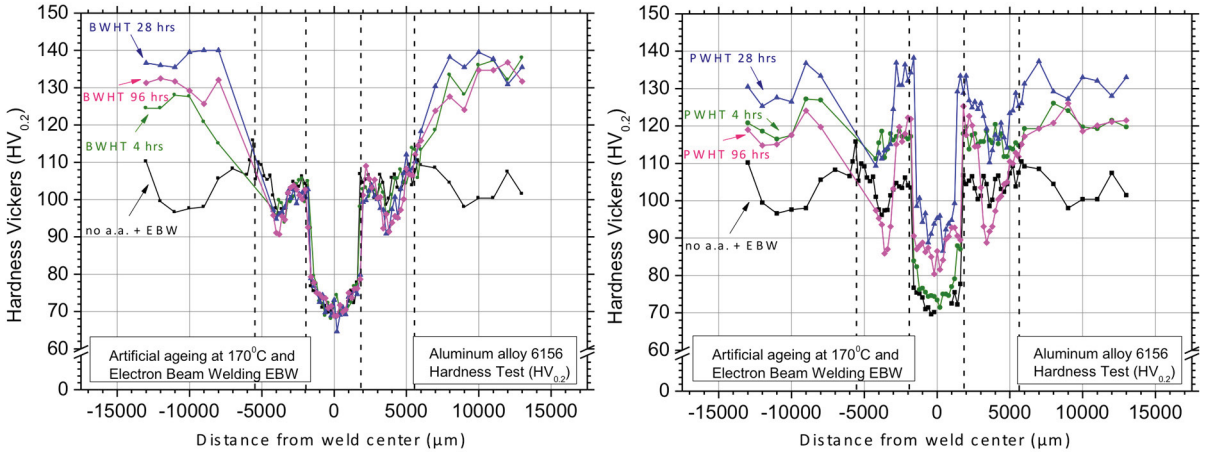

Fig. 2. Hardness Vickers measurements across the welded joint with artificial ageing (a) before; (b) post to the electron beam welding process.

3.2. Tensile test results

Typical engineering stress-strain tensile curves are presented in Fig. 3a for the specimens having heat treatment before the welding process (BWHT). The respective curves of unwelded specimens with the same artificial ageing times are presented in the same figure for comparison purposes. Reference specimens of AA6156-T4 exhibits high

tensile ductility (A_f > 20 %). After 4 hours artificial ageing at 170ºC, elongation at fracture was decreased by 5 %, while tensile ductility reached 12 % after 96 hours artificial ageing. Ultimate tensile strength takes the highest value after 28 hours artificial ageing that corresponds to the peak ageing condition. It seems that ductility decreases and strength increases with increasing ageing time up till peak-ageing condition. Comparing the unwelded artificially aged specimens with the respective BWHT specimens, it is observed that there is an obvious decrease in ultimate tensile strength and elongation at fracture that will be analyzed in the next section. The respective results for the heat treated specimens post to the welding process (PWHT) can be seen in Fig. 3b against the same artificial ageing conditions in unwelded specimens. Artificial ageing after the welding process seems to increase the strength properties of the joint mainly due to the precipitation of the second-phase precipitates. The effect on each tensile mechanical property will be discussed in the following.

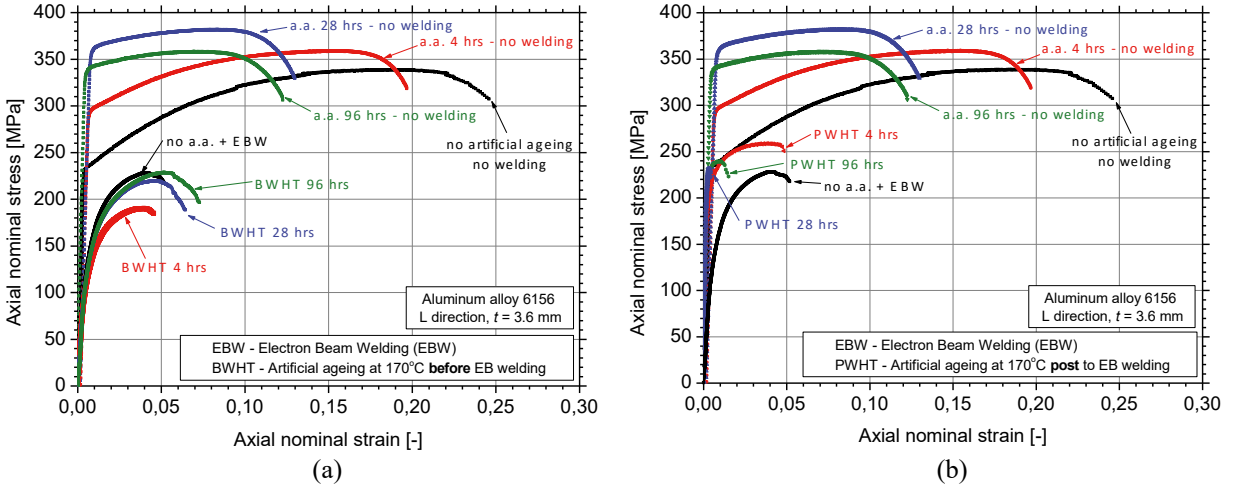

Fig. 3. Typical tensile flow curves of artificial ageing of aluminum alloy 6156 at 170ºC with and without electron beam welding with artificial ageing heat treatment (a) before EB welding; (b) post to EB welding process.

3.2.1. Conventional yield stress

Conventional yield stress $R_{p0.2\%}$ results are summarized in Fig. 4, where the calculations were based on the nominal cross - section of the specimens (engineering stress values). The results of the welded specimens were plotted against the respective unwelded specimens for various artificial ageing times at 170 ºC ageing temperature. The investigated specimens corresponded to all regions of heat treatment, including under-ageing (UA) at 4 hours, peak-ageing (PA) at 28 hours and over-ageing (OA) at 96 hours conditions. The available experimental test results were simply interpolated with the aid of a B-Spline curve (eye-catch) in order to roughly assess the effect of each process parameter. The observed yield stress increase with increasing heat treatment time, is well known phenomenon that is achieved by the precipitation of finely dispersed second-phase particles of β'' phase (Mg_2Si) in the aluminum matrix of the alloy. It is worth noticing that the welding process in T4 condition decreases the yield stress by almost 100 MPa, which corresponds to an approximate 38 % decrease.

As previously mentioned in hardness measurements section, dissolution of any formed particles and grain structure takes place in the fusion zone. Therefore, any formed precipitates in the microstructure of the alloy (e.g. BWHT specimens) are dissolved in the matrix that results in the same microstructure in the fusion zone after the welding process. Therefore the fusion zone that corresponds to the weakest ligament of the joint as already seen by the hardness measurements controls the maximum stress level of the joint until fracture. This means that despite the former ageing condition of the specimens, after welding the yield stress of the joints are more or-less- the same, without any major deviations from the welded specimens without any prior artificial ageing before EB welded. This was not the case for the PWHT specimens that had artificial ageing post to the welding process. Yield stress continuously increases with increasing artificial ageing time (Fig. 4a). This is due to the precipitation of these particles within the fusion zone that again controls fracture of the joint. It is also worth noticing the increase in $R_{p0.2\%}$ values

of the PWHT specimens that follows the trend with the yield stress increase in the unwelded specimens (supporting further the argument that this strength increase in mainly attributed to the precipitation within the fusion zone).

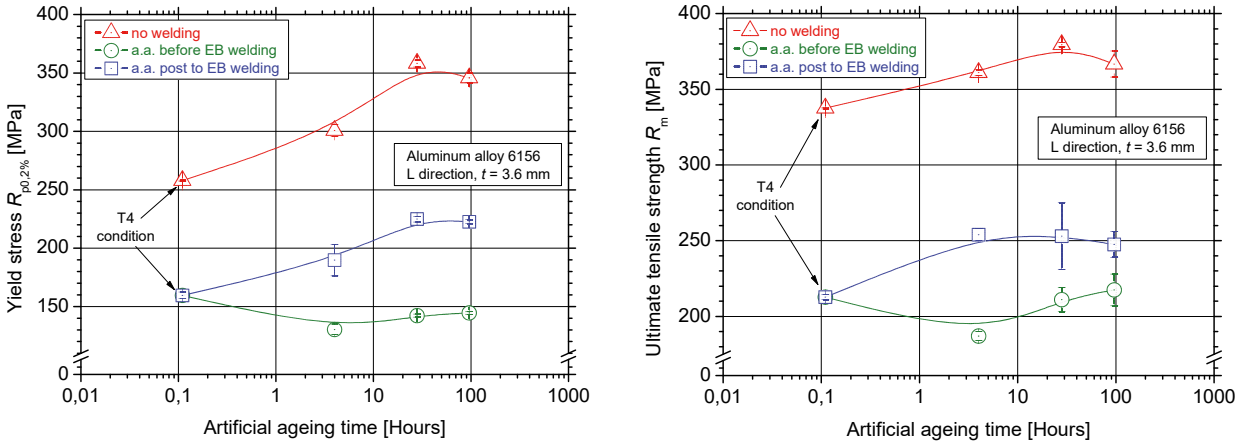

Fig. 4. (a) Yield stress $R_{p0.2\%}$; (b) ultimate tensile strength R_m values for the different investigated artificial ageing heat treatment conditions.

3.2.2. Ultimate tensile strength

Fig. 4b summarizes the ultimate tensile strength values (average value and standard deviation) as a function of artificial ageing time at 170ºC. Ultimate tensile strength R_m seems to have similar behavior with the conventional yield stress reported in the previous figure. It is worth noticing that the welding process in T4 condition decreases ultimate tensile strength by almost 125 MPa that corresponds to more than 35 % decrease. For the case of the unwelded specimens (red triangles), the trend for R_m is similar to that of $R_{p0.2\%}$ for increasing ageing time. The same arguments for dissolution/precipitation of the second-phase particles are also valid for the case of ultimate tensile strength, since they play a critical role on the strength properties of the welded joints.

3.2.3. Elongation at fracture

Average values of elongation at fracture for the investigated artificial ageing times at 170ºC can be seen in Fig. 5. For the specimens without welding the elongation decreased from 26 % to 12 % after 96 hours of artificial ageing. This ductility decrease was expected, as according to the literature in all precipitation-hardened aluminum alloys an increase in strength is always redeemed by an essential loss in ductility and vice versa, e.g. Hatch (1984). Obviously

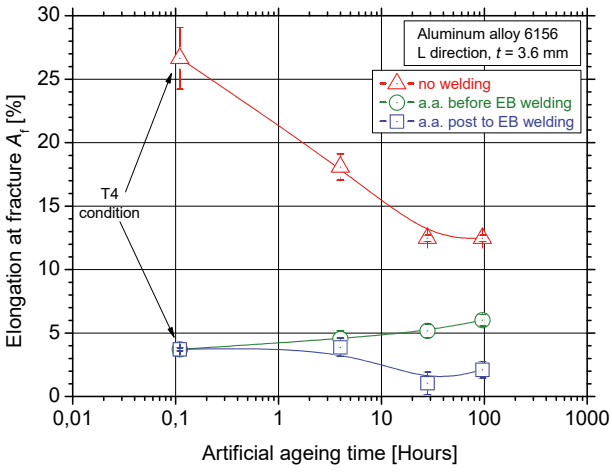

Fig. 5. Elongation at fracture A_f values for the different artificial ageing conditions with and without electron beam welding of AA6156.

this is due to the formed obstacles (precipitations) to the movement of dislocations; the latter are formed due to artificial ageing and the maximum strengthening point of the alloy is always accompanied by the lowest capacity of the material for plastic elongation (tensile ductility). The welding process in the T4 condition essentially decreased tensile ductility from approximately 26 % to 4 %. Artificial ageing plays also an important role in the ductility properties. Though in the overageing condition the unwelded specimens presented low ductility and around 12 %, the specimens with artificial ageing before the welding (BWHT) showed the highest ductility and around 6 % that is almost 50 % efficiency in the joining process. Future research will be conducted to explain the increased ductility on the microstructural level. On the contrary, the specimens with artificial ageing post to welding (PWHT) presented lower elongation at fracture that the T4 condition and around 2 %. This can be interpreted by the precipitation of the strengthening phase within the fusion zone that locally increases the strength properties and decreases the ductility potential of the welded joint.

4. Concluding remarks

Aluminum alloy 6156 electron beam joints were artificially aged before and after the welding process; ageing before the welding process results in the formation of Mg_2Si precipitates according to the different ageing condition. The welding process dissolute all the formed precipitates within the fusion zone and enhance the ductility on the expense of strength properties of the welded joints. Over-ageing before welding gave the best results in tensile ductility properties; ageing after the welding process had the opposite effect between strength and ductility properties. Small ageing time is recommended (under-ageing condition) to increase the strength properties of the welded joint.

Acknowledgements

The authors would like to thank Dr. Nikolai Kashaev and Stefan Riekehr from Materials Mechanics / Institute of Materials Research in Helmholtz Geesthacht Zentrum for conducting the hardness measurements as well as for the fruitful discussions on the tensile test results of this article.

References

Dif, R., Bès, B., Ehrström, J. C., Sigli, C., Warner, T. J., Lassince, P., Ribes, H., 2000. Understanding and modeling the mechanical and corrosion properties of 6056 for aerospace applications. Materials Science Forum, 331-337, 1613-1618.

Jin, K., Deng, Y. L., Zhou, L., Wan, L., Zhang, X. M., 2011. Investigation on artificial aging and creep aging of 6156 Aluminum Alloy. Journal of Aeronautical Materials, 31, 18-22.

Hatch, J. E., 1984. Aluminum: Properties and physical metallurgy. American Society for Metals, 233-234.

Lequeu, Ph., Lassince, Ph., Warner, T., 2007. Aluminum Alloy Development for the Airbus A380 – Alcan Aerospace 6156-T4/T62 fuselage clad sheets. Advanced Materials & Processes, 165, 41-44.

Lin, L., Zheng, Z., Li, J., 2012. Effect of aging treatment on the mechanical properties and corrosion behavior of 6156 aluminum alloy. Rare Metal Materials and Engineering, 41, 1004-1009.

Morgeneyer, T. F., Starink, M. J., Sinclair, I., 2006. Experimental analysis of toughness in 6156 Al-alloy sheet for aerospace applications. Materials Science Forum, 519-521, 1023-1028.

Morgeneyer, T. F., Starink, M. J., Wang, S. C., Sinclair I., 2008. Quench sensitivity of toughness in Al alloy: Direct observation and analysis of failure initiation at the precipitate-free zone. Acta Materialia, 56, 2872-2884.

She, L., Zheng, Z., Zhong, S., Wu, Q., Li, H., 2013. Effects of aging treatments on tensile properties and fracture toughness of AA6156 aluminum alloy. Rare Metal Material and Engineering, 42, 2163-2168.

Stefanou, G., Migklis, E., Kourkoulis, S., Alexopoulos, N. D., 2014. Mechanical behaviour of aeronautical aluminum alloy 6156 for different artificial aging conditions. In: Proceedings of International Symposium on Aircraft Materials ACMA 2014, Marrakech, Morocco, 23-26.

Zhang, H., Zheng, Z., Lin, Y.,Luo, X., Zhong, J., 2012. Effects of Ag addition on the microstructure and thermal stability of 6156 alloy. Journal of Materials Science, 47, 4101-4109.